Investigation of the Dynamics and Kinetics Involved in Saline Aerosol Generation Under Air Erosion of Pure and Contaminated Halide Salts.

Investigation of the dynamics and kinetics involved in saline aerosol generation under air erosion of pure and contaminated halide salts

Ion Sandu[a], Romeo Iulian Olariu[b], Ioan Gabriel Sandu[c], Catalina Stirbu[c], Constantin Pascu[d], Viorica Vasilache[a], Davide Vione[e], Cecilia Arsene[b,*]

[a]„Alexandru Ioan Cuza" University of Iasi, Environmental Science School, 11 Carol I, 700506 Iasi, Romania

[b]„Alexandru Ioan Cuza" University of Iasi, Faculty of Chemistry, 11 Carol I, 700506 Iasi, Romania

[c]„Gh. Asachi" Technical University of Iasi, 71 D. Mangeron, 700050 Iasi, Romania

[d]Romanian Inventors Forum, 3 Petru Movila Street, 700089 Iasi, Romania

[e] Dipartimento di Chimica, Università di Torino, Via Pietro Giuria 5, 10125 Torino, Italy

[*]Corresponding author. Tel.: +40 232 201354; Fax: +40 232 201313

E-mail address: carsene@uaic.ro (Cecilia Arsene)

Abstract

This study presents results from an investigation of the dynamics and kinetics involved in saline aerosol generation under air erosion of pure and contaminated halide salts. Investigations have been performed in a microhalochamber filled with active efflorescent pure or doped NaCl salt granules. The performed work allows the suggestion that pure NaCl salt presents the highest potential to generate saline aerosols. The generation capacity of saline aerosols decreased in doped NaCl, and the efficiency of the doping salts to inhibit aerosol generation was in the order (KI + KCl) > KI ≈ KBr > KCl > $CaCl_2$. Emission/erosion rate constants (min^{-1}) were estimated by applying a simple kinetic treatment to the experimental data set (i.e. trends of $\ln([S_0]/[S])$ *vs*. time, where S represents the salt). The pseudo-first order erosion rate constant value (k_e), characteristic of the emission/erosion of aerosol from salt granules, decreased in the order $NaCl_{\text{pure crystallite}} > NaCl_{\text{doped with CaCl2 or KCl salts}} > NaCl_{\text{doped with KBr or KI salts}}$. For the doping salt the emission/erosion rate constants varied in the order: $k_{e(KI)} < k_{e(KBr)} < k_{e(KCl)} < k_{e(CaCl2)}$. The emission/erosion process is most probably controlled by the morphology of the used salt granules. The latter would be related to the solubility of the doping salt, the radii of the involved ions and the properties of the saline aqueous solutions that are used to obtain active efflorescent salt granules. Such properties could affect the surface enrichment of NaCl and of the doping salt, because surface composition is expected to play an important role at least in the first stage of the erosion process. The obtained results may have relevant implications in both atmospheric and medical fields.

Keywords: respiratory disease, aerosol generation, dynamics, erosion, dry air, saline aerosols, pure and doped NaCl salt.

1. Introduction

Sodium chloride (NaCl) aerosols, on their own or in mixture with other halides, are usually polydisperse systems with individual components in the size range from Aitken nuclei (particle radii smaller than 0.1 μm) to large (particle radii between 0.1 and 1 μm) and giant (particle radii larger than 1 μm) particles. However, in the aerosol size range spectrum, Junge and Jaenicke (1971) report about a concentration maximum of particles around 0.001 μm radius, supporting the idea of a dynamic equilibrium in the size distribution of the aerosol. The observation of Junge and Jaenicke (1971) was later confirmed by the data of Haaf and Jaenicke (1980), who observed a bimodal distribution in the Aitken range of atmospheric aerosols. According to Whitby (1978) and depending on the aerosol production mechanisms, aerosols are classified into nucleation (particle diameter <0.1 μm), accumulation (particle diameter in the 0.1 - 2 μm size range) and coarse (particle diameter larger than 2 μm) mode particles. Hygroscopicity is an important aerosol property, especially in aerosols that contain water-soluble substances. Many inorganic salt aerosols are hygroscopic by nature and exhibit the property of deliquescence in humid air (Tang, 1996). Tang (1996) also underlined that when the relative humidity in the surrounding air reaches the deliquescence point, a particle rapidly takes up water and becomes a saturated droplet. The droplet thus formed usually does not recrystallize when the relative humidity falls below the deliquescence point. However, it is generally admitted that the hygroscopicity of inorganic aerosols is directly interrelated to the initial particle size and relative humidity (Hu et al., 2010). Furthermore, evaporation and growth of multicomponent aerosols can be directly linked to the use of a laminar flow humidifying system, by controlling the vapor partial pressure along the humidifying tube in a known manner (Kreidenweis et al., 1987). Moreover, thermodynamic analysis has shown that phase partitioning of multicomponent aerosol particles occurs during crystallization, and particles dried from multicomponent aqueous aerosols do not have a homogeneous chemical morphology except at the eutonic point (the point on a phase diagram where the mixture of chemical compounds has a single chemical composition that solidifies at a lower temperature than any other composition) (Ge et al., 1996).

Specific physico-chemical properties of selected saline aerosols represent key points for some of their multiple practical applications (e.g. prophylaxis and treatment of respiratory diseases, improvement of the cardio-respiratory parameters, purification and air quality improvement) (Chervinskaya & Zilber, 1995; Hedman et al., 2006; Sandu et al., 2010a; Cho et al., 2011). In particular, natural or generated saline sodium chloride (NaCl) aerosols have considerable importance in creating therapeutic environments (Smaldone et al., 1989; Beck-Broichsitter et al., 2009; Horowitz, 2010). It is believed that an important characteristic of saline aerosols is represented by the critical limit of the relative humidity that controls the formation of condensation nuclei through the deliquescence process (McGraw & Lewis, 2009). Up to now much work was devoted to the hygroscopicity and the dynamic shape of NaCl aerosols (Wise et al., 2007). Organic compounds may affect the hygroscopic properties of NaCl aerosol particles at relative humidity in the range of 30-90% (Hansson et al., 1998). For NaCl nanoparticles, there is suggestion that the dynamic shape is strictly related to the drying rate (Wang et al., 2010). Moreover, there are also reports about theoretical calculations on the total and regional depositions of dry NaCl aerosols in the human respiratory tract for initial particle diameters ranging from 0.01 to 10 μm (Xu & You, 1985). A theoretical model has been used to predict the efflorescence relative humidity (ERH) of NaCl particles in sizes ranging from 6 nm to 20 μm (Gao et al., 2007). Gao et al. (2007) found that when the NaCl particles are larger than 70 nm, the ERH decreases with decreasing dry particle size and reaches a minimum around 44-45% RH. In contrast, for particles smaller than 70 nm, the ERH increases with decreasing dry particle size because of the Kelvin effect. Usually, time variability in the chemical composition of NaCl aerosols seems to be induced by the interaction with water dipoles and other ions or particles during their structural reorganization. However, there is suggestion that the composition correlates with the aerosols shape and size (Sandu et al., 2003; 2010b; 2010c).

Submicron dispersions of dried saline aerosols are mainly used for therapeutic purposes (Mendes et al., 2009), while for ambient environments dried aerosols are of high interest (Stanier et al., 2004). The last situation is often associated to conditions equivalent to the "clean air effect". In practical applications, the efficiency of aerosols and nanoparticles in prevention, care and cardio-respiratory function improvement is believed to depend on aerosols life time, abundance and shape, which should be very strictly controlled (Tang et al., 2006; King & Zayas, 2007; Beck-Broichsitter et al., 2009). There are reports on the effect of salt chamber treatment on bronchial hyperresponsiveness in asthmatics (Hedman et al., 2006) and on the use of specially designed halochambers, constructed to simulate the microclimate

of salt mines (Chervinskaya & Zilber, 1995). Javaheri et al. (2013) suggested that when hygroscopic aerosols are inhaled, the size and temperature of the dispersed droplets (as well as the temperature and moisture content of the carrier gas) may change due to heat and mass transfer between the dispersed phase and the carrier gas, and also between the gas and the walls of the respiratory tract. The lowest deposition fraction in the extra-thoracic region and the highest deposition fraction in the alveolar region corresponded to droplets with low mass fraction, inhaled with an helium–oxygen mixture.

The present paper reports about the experimental evidence of the influence of doping Na, K and Ca halides on the generation mechanism of saline aerosols. The obtained results may have implications in the optimization processes of particles generation by dynamic halochambers used in medical applications.

2. Experimental

Salts used in saline aerosol generation

Reagent-grade salts from Sigma-Aldrich were used in the present investigation. Pure and doped NaCl salts were obtained by recrystallization from supersaturated aqueous solutions of binary salts mixed in different ratios. The contamination limit with other salts was established according to information related to the chemical composition of natural mine salt often used in saline aerosol generation for therapeutic purposes (Sandu et al., 2010b,c). The chemical composition of the investigated samples consisted of 100% NaCl (P_0), 95% NaCl + 5% KCl (P_1), 95% NaCl + 5% KI (P_2), 95% NaCl + 5% KBr (P_3), 90% NaCl + 5% KCl + 5% KI (P_4) and 95% NaCl + 5% $CaCl_2$ (P_5). Salt mixtures wetted with ultrapure water (18.2 MΩ·cm resistivity, produced by a PURELAB Option-Q system) were gently mixed to obtain supersaturated slurries which were further subjected to drying for 2 - 3 h in an oven at 80 °C. The generated salts, extruded and finally conditioned in the form of efflorescent granules, were stored under dry conditions in airtight polyethylene bags until experimental investigations. More details about the salts generation procedure are presented elsewhere (Sandu et al., 2013). A precisely weighted aliquot (60 g) of activated efflorescent granules was used to fill up a microhalochamber designed for experimental investigations.

Generation of pure and doped saline aerosols

The effect of doping with other salts on the generation rate of saline aerosols was investigated by an instrumental setup including as major constituents a dried air pump, a microhalochamber and a purging unit. Saline aerosols were generated by drawing dried synthetic air at a flow rate of 1.8 L min^{-1} through the filled microhalochamber. Size range

characteristics of the aerosol particles generated under such conditions are elsewhere presented (Sandu et al., 2013). Saline aerosols generated from 60 g of pure or doped NaCl granules (samples P_0 – P_5) were collected in 100 mL ultrapure water by purging continuously in an impinger the effluent from the microhalochamber. The saline aerosol mixture was bubbled for 30 minutes for three separate replicates (P_{0i} – P_{5i}, where i = 1, 2 and 3). Moreover, the mixture was bubbled for an hour for P_{04} – P_{54} samples (i = 4), three hours for P_{05} – P_{55} (i = 5), six hours for P_{06} – P_{56} (i = 6), 10 hours for P_{07} – P_{57} (i = 7), 15 hours for P_{08} – P_{58} (i = 8), and 20 hours P_{09} – P_{59} (i = 9). For the P_{08} – P_{58} and P_{09} – P_{59} samples, continuously exposed for longer periods at a 1.8 L min^{-1} flow rate, the final volume of 100 mL was kept at a constant value by adding at the end of the experiment between 1 and 1.5 mL of ultrapure water, depending upon the time scale of the experiment (i.e. 15 and, respectively, 20 hours). However, the relatively slow flow rate used for purging purposes in the present work allowed the vapor pressure of the system to adequately equilibrate. Moreover, for the entire set of experiments the environmental conditions were strictly controlled, to keep the temperature and relative humidity at suitable values. Taking into account the aspects mentioned before, a mathematical correction was not applied during the quantification procedure.

Ion chromatographic analysis of the generated pure and doped saline aerosols

Ion chromatography was used to assess the chemical composition of the generated saline aerosol particles. Analysis of the chemical parameters of interest (cations and anions) was carried out on each 100 mL aqueous solution collected from the impinger. Analysis of sodium (Na^+), potassium (K^+), calcium (Ca^{2+}), chloride (Cl^-) and bromide (Br^-) ions was performed on an ICS DIONEX 3000 ion chromatograph. Separation and quantification of the water-soluble anions was achieved with an IonPac AS22 (4×250 mm) analytical column and an ASRS 300 (4 mm) auto-suppressor, while an IonPac CS17 (4×250 mm) analytical column and a CSRS 300 (4 mm) auto-suppressor were used for the analysis of the water-soluble cations. Calibration curves for the target anions and cations were performed on each analysis day. Before the injection of each sample replicate, one blank solution (ultrapure water) was injected and analyzed. The mobile phase for cations analysis consisted of 6 mM methane sulphonic acid (MSA) at a flow rate of 1 mL min^{-1}, while that for the anions consisted of a mixture of 1.4 mM Na_2CO_3 and 0.4 mM $NaHCO_3$ at a flow rate of 1.2 mL min^{-1}. The reagents used in the analysis were of analytical grade and working standard solutions were prepared in ultrapure water.

3. Results and discussion

Ion chromatography was used to explore the chemical composition of the saline aerosols formed under air erosion of pure and doped halide salts. Data concerning the target water-soluble ions in samples P_{0i} to P_{5i} were processed, to investigate the effect of salt doping in saline aerosols generation. The analysis of both cations and anions yielded very similar information, thus the following discussion only focuses on cations. Fig. 1 presents the time trends of the saline aerosol concentration, derived as the sum of the concentrations of the interest species in each series of samples. For instance, in the case of NaCl + KCl, the reported concentration is $C = [Na^+] + [K^+]$.

Data in Fig. 1 clearly show that the doping of NaCl with other salts is highly affecting the abundance of the saline aerosol particles. A considerable decrease in saline aerosol generation is observed upon doping, and aerosol generation follows the order NaCl > NaCl + $CaCl_2$ > NaCl + KCl > NaCl + KBr ≈ NaCl + KI > NaCl + KCl + KI. It appears that doping with $CaCl_2$ decreases the aerosol concentration down to almost one quarter of the value obtained with pure NaCl, while under other doping conditions (e.g. NaCl doped with KI and KBr) the aerosol concentration may be decreased by over 90% (except for the longest bubbling time).

The influence of the different doping salts is highlighted with more detail in Fig. 2, which reports for each experiment the time trend of the concentrations of all the relevant cationic species. The data of Fig. 2 show that the fraction of the doping ions, compared to Na^+, is always higher in the aerosols than in the source solids. This is particularly true of samples P_1, P_4 and P_5 that contain KCl, KCl + KI and $CaCl_2$, respectively, as doping salts. In the case of P_5 one should consider that, because of charge issues, a Ca^{2+} ion would replace two Na^+ ions in both the solid lattice and the solution. Indeed, the normality of Ca^{2+} in solution (product of concentration times charge) is actually very similar to that of Na^+. In the case of P_2 and P_3 (respectively containing KI and KBr) the fraction of the doping ions in solution, although higher than in the original solid, is still considerably lower compared to the Na^+ one. To explain the fact that the fraction of the doping ions is higher in solution than in the original solid, one can suppose that the formation of solid NaCl from supersaturated solutions would tend to expel extraneous ions out of the NaCl lattice. Therefore, either NaCl grows around the other salt, or the other salt forms a deposit on the NaCl surface. Possibly, if solubilities are not much different, the latter happens to some extent in all the cases and air erosion, which operates first of all on the surface of the salt granules, removes solid material that is enriched in doping salts and finally reaches the impinger.

Therefore, one should assume that the granules of the doped salts are not homogeneous. Another reason for this to happen is the accumulation of the most soluble compounds at the granule surface. Indeed, the most soluble species would be the last to precipitate from the supersaturated solutions, used to prepare the granules for the erosion tests. A very important role might also be played by the aerosol generation procedure and by the specific structural properties of the doped NaCl granules used to generate the aerosol particles. A size-dependent hygroscopic property of NaCl particles is reported in the literature (Park et al., 2009). Park et al. have observed that the growth factor (GF) of the particles decreased with decreasing size, and the extent of the GF cessation was greater than theoretically predicted with the Kelvin correction. Moreover, the GF of furnace-generated NaCl nanoparticles (having pores and aggregate shape) was smaller compared to atomizer-generated particles that were almost perfectly cubic. Park et al. (2009) also report that the GFs of atomizer-generated particles of KCl, $MgCl_2$ and $CaCl_2$ are independent of particle size. Sullivan et al. (2009) report that the apparent hygroscopicity of various minerals is primarily controlled by their specific solubility, and that a significant increase in hygroscopicity is caused by mixing soluble hygroscopic materials.

The solubility at 25°C of the inorganic salts of interest in the present study, as given in the CRC Handbook of Chemistry and Physics (88^{th} Edition), varies in the following order: $CaCl_2 > NaCl \approx KCl$ (i.e., $813 > 360 \approx 355$ g L^{-1}). Since the hygroscopicity of pure or doped NaCl granules is expected to vary in a similar manner, it is possible that this property also controls the emission capacity of the saline aerosols. The latter is for instance lower for P_1 (NaCl doped with KCl) and P_4 (NaCl doped with KCl and KI) compared to P_5 (NaCl doped with $CaCl_2$), as shown in Fig. 1. It is also worth mentioning that, in the case of P_5, the contribution of Na^+ alone to the generation of the saline aerosol is lower compared to P_1 and higher compared to P_4. This issue could be consistent with a surface accumulation of $CaCl_2$ because of its higher solubility. In other two situations, *i.e.* samples P_2 and P_3 (where KI and KBr were used as doping salts, respectively), the contribution of K^+ to the saline aerosol is much smaller compared to Na^+. Moreover, in samples doped with KI (P_2, P_4) the total aerosol emission capacity seems to be significantly lower compared to sample P_3, doped with KBr (see Fig. 1).

Further indications could be obtained by a kinetic treatment of the experimental data. In the present case, let S be the reactant in the form of pure or doped NaCl salt granules, and P the product in the form of saline aerosol particles formed by the erosion of the granules (as a

consequence of continuous blowing of air through a granules-filled cartridge). The process can be described as follows:

$$\text{S (pure or doped NaCl salt granules)} \xrightarrow{k_e} \text{P (saline aerosols)} \qquad (1)$$

where k_e, called the erosion rate constant, is referred to both the disappearance of S and the formation of P. Using a simple kinetic formalism developed for a first-order reaction, the values of k_e can be experimentally deduced. Note that the rate of S disappearance (d[S]/dt) is negative as it indicates consumption of the reactant (i.e. NaCl salt granules), while the rate of P formation (d[P]/dt) is positive. Because S can only give P in a 1:1 ratio, the absolute values of the two rates are necessarily equal. The entire kinetic formalism can be described by equations (2) – (5):

$$\text{erosion / formation rate} = -\frac{d[S]}{dt} = \frac{d[P]}{dt} \qquad (2)$$

$$-\frac{d[S]}{dt} = k_e \times [S] \qquad (3)$$

According to the integrated rate law:

$$\ln[S] = -k_e \times t + \ln[S]_0 \qquad (4)$$

$$\ln\frac{[S]_0}{[S]} = k_e \times t \qquad (5)$$

By plotting the experimental values of $\ln([S]_0/[S])$ vs. time, it is possible to determine the erosion rate constant k_e as the line slope. In our case, the logarithm to the base e or natural logarithm has been applied to the data set of halide decay induced by the erosion of the efflorescent salt granules. The amount of the eroded salt has been indirectly derived from the concentration of the ions quantified by ion chromatography. The following assumptions have been made:

$$S = S_0 - S_e \qquad (6)$$

where

S - the amount of the solid reactant remaining after a certain time of continuous air blowing through the granules-filled cartridge (pure or doped NaCl salt granules)

S_0 - the initial mass, m_0 = 60 g, of the granules-filled cartridge (pure or doped NaCl salt granules)

S_e - the eroded mass, m (g), determined by the following formula

$$m(g) = C \times V \times \frac{M_S}{A_I} \times 10^{-6} \qquad (7)$$

with

C - the concentration of the specific ion in μg mL^{-1}

V - the 100 mL volume of ultrapure water in the impinger

M_S – the molar mass of the interest salt in g mol^{-1}

A_I – the ionic mass of the interest ion in g mol^{-1}.

The eq. (7) applies to both NaCl and the doping salt(s) (KCl, KBr, KI, $CaCl_2$). The relevant plots for the investigated systems in terms of $\ln([S]_0/[S])$ vs. time are shown in Fig. 3. It can be seen that they consist of a series of linear trends with different slopes, which suggests that different steps (each with peculiar reaction kinetics) are followed when varying the reaction time. In the case of pure NaCl aerosols, a two-stage generation mechanism appears to be operational. Under all the other doping conditions, the generation of saline aerosol would occur in three steps.

In the case of NaCl aerosols produced from pure NaCl salt, the suggested process would involve a gradual change from an emission controlled by the material at the surface, up to an emission pathway controlled by the material that is found deep inside the salt. The homogeneity and porosity degrees of the salt (surface *vs.* bulk) as well as the occurrence of particles with different size could influence the kinetics of air erosion and would contribute to the observed behavior. For the doped salts, the three-step process might be a result of contributions from external surface emissions (I), emissions from the cavities located immediately near the surface (II) and residual emissions from both external and internal cavities (III). These processes would involve a decrease in the erosion rate constant in the order (I) > (II) ≥ (III). Moreover, for the doped salts, the non-homogeneity and higher porosity induced by the ionic radii of the doping elements (Huheey et al., 1993) might be directly related with the occurrence of several erosion steps. It should be stressed that, for the three-step process, the second stage is usually described by the linear regression analysis of only three to four points. The correlation would be statistically significant, at 95.4% confidence level and a freedom degree of 2, if the Pearson coefficient (r) takes the value of 0.950. In the present experimental investigations, for the second stage r is always higher than 0.97. Under these circumstances it appears that the second stage represents a genuinely distinct process, and not only a transition between the initial and the final dynamic erosion regime.

If this is the case, it is possible to account for the data presented in both Fig. 2 and Fig. 3. In particular, samples P_2 (NaCl + KI), P_3 (NaCl + KBr) and, to a lesser extent, P_1 (NaCl + KCl) and P_4 (NaCl + KCl + KI) have NaCl as the main eroded salt, while in the case of P_5 the doping salt ($CaCl_2$) is eroded to a comparable or even higher extent than NaCl. Generally speaking, it is possible to hypothesize that the chemical composition of the generated aerosols is controlled by salt features such as solubility, hygroscopicity and ionic radii. When NaCl is doped with $CaCl_2$ and KCl (samples P_5, P_1 and P_4), solubility seems to play an important role and one might assume that $CaCl_2$ and KCl would be preferentially located at the surface of the granules undergoing erosion.

As far as the ionic radii are concerned, they vary in the order $I^- > Br^- > Cl^-$ for anions and in the order $K^+ > Ca^{2+} > Na^+$ for cations (Huheey et al., 1993). Therefore, potassium iodide and potassium bromide (present in samples P_2 and P_3) involve species with the largest ionic radii on the side of both anions and cations. In the case of a 1:9600 NaBr-NaCl aqueous solution evaporated to 1:400 NaBr-NaCl ratio, the surface of the generated deposit of salts can be 35-fold enriched in NaBr but only for a specific size fraction (Zangmeister et al., 2001). Moreover, large areas of the salts deposit surface contain NaCl with no detectable NaBr. Zelenov et al. (2008) brought evidence of the fact that an important fraction of the surface area in a X/NaCl binary mixture can be occupied by the X doping salt, where X can be NaBr, NaI, $MgCl_2 \times 6H_2O$ or $MgBr_2 \times 6H_2O$. Such an issue might explain the enrichment of the doping salts in the aerosol compared to the initial granules, as found in the present work in all the relevant experiments. The extent of the enrichment, which is for instance very marked for $CaCl_2$ and much less evident for KBr or KI, could then be influenced by solubility issues.

Table 1 reports the features of the regression lines relevant to the experimental data of Fig. 3, as well as their correlation coefficients. The calculations consider only the data derived from cation analysis. The data of Table 1 correspond to a three-stage aerosol generation process. For the first stage, application of equation (5) to the experimental data allowed the quantification of the emission/erosion rate, k_e in min^{-1} units. The value of k_e is the highest in the case of saline aerosols generated from pure NaCl. Passing from pure to doped salt, the k_e values decrease in the order $NaCl_{\text{pure crystallite}} > NaCl_{\text{doped with CaCl2 salts or KCl}} > NaCl_{\text{doped with KI or KBr salts}}$. When focusing on the doping salt, the emission/erosion rates vary in the following order: $k_{e(KI)} < k_{e(KBr)} < k_{e(KCl)} < k_{e(CaCl2)}$. It is quite likely that the elevated erosion/emission rate for $CaCl_2$ is accounted for by the fact that this salt is preferentially located at the surface of NaCl crystals. Arima et al. (2009) studied the adsorption and deliquescence of water on alkali halide nanocrystals (KBr, KCl, KF, NaCl), supported on SiO_2. They observed that for

KBr, KCl and NaCl the droplets exhibited a negative surface potential relative to the surrounding region. This was considered as an indication of the preferential segregation of the anions at the air/solution interface. Segregation to the solution surface was also reported for Br^- and I^- in mixed NaBr/NaCl or NaI/NaCl aqueous systems (Ghosal et al., 2005). Under these circumstances, it is expected that the crystallysation/recrystallisation process is directly influenced by the properties of the saline aqueous solutions.

No attempt will be made here to account for the regression characteristics of the second and the third stage of the erosion process, because several additional phenomena may occur after the first stage and they would complicate the overall framework. However, it is very likely that the aerosol generation process is strictly controlled by the morphology of the used salt granules. The surface layer of the NaCl salt is probably enriched with the doping salt in most of the investigated cases, a phenomenon that could depend on the water solubility of the salt. Important exceptions are KBr and KI, probably because of the large radii of their ions. Under these circumstances, aerosol generation would be controlled by emission/erosion either from the surface, or from labile internal crystallites within the used salt granules.

We would like to point out that the aerosol generation technique used in the current work is stated as a reliable source of particulate matter (Gill et al., 2006), and the choice was made to employ sample powders with a composition that mimics the state in which they exist in nature. Interesting supplementary approaches for further study could consist into extensively sieving or otherwise pre-separating the source constituents into several size-fractions prior to the erosion exposure. This may lead to the removal of weakly bonded or surface-coagulated small particles that could be more likely responsible for the first slope dynamic profile. Our previous studies (Sandu et al., 2013) suggest that in the given experimental conditions the quantity of huge micro-particles (>1 μm) emitted right after the cartridge is slightly lower in the case of NaCl 100% as compared with the doped salts. Therefore, the hypothesis of higher erosion rates due to larger NaCl wind-swept particles seems discarded. In contrast, the micronic and sub-micronic particles follow an erosion surface passivation profile that seems to support the above hypothesis. An additional approach to sample pre-treatment that could avoid the surface enrichment with doping salts may consist into the generation of pure individual efflorescent salt granules and subsequent mechanical homogenization at the chosen mixing ratios. The dissimilarities between the two types of sample preparation (co-crystallization versus mechanical mixing) could then be assigned to surface enrichment effects or structural dimness of the mainly eroded saline efflorescent crystals. (a deleted sentence here)

The air flow rate into the filtering cartridge could equally represent an interesting erosion parameter to be taken into account in further studies, which could bring supplementary information onto the mechanism of material removal (Alfaro & Gomes, 2001). As a key result, the current study opens new research perspectives into the field, requiring further descriptions of the material removal mechanism by air erosion, including the size, shape, specific surface and porosity characterization of the formed efflorescent conglomerate.

Conclusions

The performed work allows the suggestion that pure NaCl salt shows the highest potential to generate saline aerosols. The aerosol generation capacity varies depending on the type of doping salt, and the aerosol generation order is $CaCl_2$ > KCl > KBr ≈ KI > (KCl + KI). Emission/erosion rates (i.e., k_e in min^{-1}) have been estimated by using a simple kinetic treatment (based on plots of $\ln([S_0]/[S])$ vs. time) applied to the data set of interest. The k_e value characteristic for NaCl emission/erosion is decreasing in the order $NaCl_{\text{pure crystallite}}$ > $NaCl_{\text{doped with CaCl2 or KCl salts}}$ > $NaCl_{\text{doped with KBr or KI salts}}$. For the doping salt the emission/erosion rates vary in the following order: $k_{e(KI)} < k_{e(KBr)} < k_{e(KCl)} < k_{e(CaCl2)}$. The emission rates of the different species from the salt granules are most likely controlled by the granule morphology, in particular as far as surface enrichment *vs*. internal composition is concerned. Morphology may be influenced by the water solubility of the doping salts, as the most soluble ones would be the last to precipitate from the solution and they would be preferentially accumulated at the surface of the granules. This feature could account for the high erosion rates of $CaCl_2$ and KCl. However, ionic radii could also play a role and salts with large ions (such as KI and KBr) could undergo a lesser extent of surface enrichment.

Additional work will be required before the experimental findings of the present work find practical applications. A major and challenging issue concerns for instance the physical stability of the saline aerosol. However, preliminary data suggest that the purity of the NaCl salt used as the basis for aerosol production could play a very important role.

Acknowledgements

R.I. Olariu and C. Arsene acknowledge the financial support for research in the field provided by UEFISCDI within the PN-II-PCE-2011-3-0471 Project, Contract No. 200/05.10.2011. The POSCCE-O 2.2.1, SMIS-CSNR 13984-901, No. 257/28.09.2010 Project, CERNESIM, is also gratefully acknowledged for the infrastructure used in this work. The authors gratefully

acknowledge the comments and suggestions of an anonymous reviewer who really helped to improve the manuscript.

References

Arima, K., Jiang, P., Lin, D.S., Verdaguer, A., Salmeron, M. (2009). Ion segregation of alkali halide nanocrystals on SiO_2. *Journal of Physical Chemistry A*, *113*, 9715-9720.

Beck-Broichsitter, M., Gauss, J., Pachaeuser, C.B., Lahnstein, K., Schmehl, T., Seeger, W., Kissel, T., & Gessler, T. (2009). Pulmonary drug delivery with aerosolizable nanoparticles in an *ex vivo* lung model. *International Journal of Pharmaceutics*, *367*, 169-178.

Chervinskaya A.V., & Zilber N.A. (1995). Halotherapy for treatment of respiratory diseases, *Journal of Aerosol Medicine: Deposition, Clearance, and Effects in the Lung*, *8*, 221-232.

Cho, H.W., Yoon, C.S., Lee, J.H., Lee, S.J., Viner, A., & Johnson, E.W. (2011). Comparison of pressure drop and filtration efficiency of particulate respirators using welding fumes and sodium chloride. *The Annals of Occupational Hygiene*, *55*, 666-680.

CRC Handbook of Chemistry and Physics (88^{th} Edition) 2007-2008, Lide, D.R. (Ed)., CRC Press.

Gao, Y., Chen, S.B., & Yu, L.E. (2007). Efflorescence relative humidity odf airborne sodium chloride particles: a theoretical investigation. *Atmospheric Environment*, *41*, 2019-2023.

Ge, Z., Wexler, A.S., Johnston, M.V. (1996). Phase partitioning of aerosol particles during crystallyzation. In Nucleation and Atmospheric Aerosols. Kulmala, M.; Wagner, P.E., eds. Pergamon, 462-464.

Ghosal, S., Hemminger, J.C., Bluhm, H., Mun, B.S., Hebenstreit, E.L.D., Ketteler, G., Ogletree, D.F., Requejo, F.G., & Salmeron, M. (2005). Electron spectroscopy of aqueous solution interfaces reveals surface enhancement of halides. *Science*, *307*, 563-566.

Haaf, W., & Jaenicke, R. (1980). Results of improved size distribution measurements in the Aitken range of atmospheric aerosols. *Journal of Aerosol Science*, *11*, 321-330.

Hansson, H.C., Rood, M.J., Koloutsou-Vakakis, S., Hameri, K., & Orsini, D. (1998) Wiedensohler. NaCl aerosol particle hygroscopicity dependence on mixing with organic compounds. *Journal of Atmospheric Chemistry*, *31*, 321-346.

Hedman, J., Hugg, T., Sandell, J., Haahtela, T. (2006). The effect of salt chamber treatment on bronchial hyperresponsiveness in asthmatics. *Allergy*, *61*, 605-610.

Horowitz, S. (2010). Salt cave therapy: rediscovering the benefits of an old preservative. *Alternative and Complementary Therapies*, *16*, 158-162.

Hu, D., Qiao, L., Chen, J., Ye, X., Yang, X., Cheng, T., & Fang, W. (2010). Hygroscopicity of inorganic aerosols: Size and relative humidity effects on the growth factor. *Aerosol and Air Quality Research*, *10*, 255-264.

Huheey, J.E., Keiter, E.A., Keiter, R.L. (1993). in Inorganic Chemistry: Principles of Structure and Reactivity, 4th edition, HarperCollins, New York, USA.

Javaheri, E., Shemirani, F.M., Pichelin, M., Katz, I.M., Caillibotte, G., Vehring, R., Finlay, W.H. (2013). Deposition modelling of hygroscopic saline aerosols in the human respiratory tract: Comparison between air and helium–oxygen as carrier gases. *Journal of Aerosol Science*, *64*, 91-93.

Junge, C., & Jaenicke, R. (1971). New results in background aerosols studies from the Atlantic expedition of the R.V. Meteor, Spring 1969. *Journal of Aerosol Scienc*e, *2*, 305-314.

King, M., & Zayas, G.J. (2007). Compositions and methods for improved mucus function. United States Patent Application Publication, 0275091 A1.

Kreidenweis, S.M., Flagan, R.C., & Seinfeld, J.H. (1987). Evaporation and growth of multicomponent aerosols laboratory applications. *Aerosol Science and Technology*, *6*, 1-14.

McGraw, R., & Lewis, E.R. (2009). Deliquescence and efflorescence of small particles. *Journal of Chemical Physics*, *131*, 194705, doi: 10.1063/1.3251056.

Mendes, P.J., Pinto, J.F., Sousa, J.M.M. (2009). Numerical simulation of in-vitro dispersion and deposition of nanoparticles in dry-powder-inhaler aerosols. *Journal of Nanoscience and Nanotechnology*, *9*, 1-7.

Park, K., Kim, J.S., & Miller, A.L. (2009). A study on effects of size and structure on hygroscopicity of nanoparticles using a tandem differential mobility analyzer and TEM. *Journal of Nanoparticle Research*, *11*, 175-183.

Sandu, I., Pascu, C., Sandu, I.G., Ciobanu, G., Vasile, V., & Ciobanu, O. (2003). The obtaining and characterization of NaCl nanocrystalline dispersions for saline type therapeutical media. I. Theoretical aspects. *Revista de Chimie*, *54*, 807-812.

Sandu, I., Poruciuc, A., Alexianu, M., Curca, R.G., & Weller, O. (2010a). Salt and human health: science, archaeology, ancient texts and traditional practices of eastern Romania. *Mankind Quarterly*, *50*, 225-256.

Sandu, I., Chirazi, M., Canache, M., Sandu, G.I., Alexeianu, M.T., Sandu, V.A., & Vasilache, V. (2010b). Research on NaCl saline aerosols I. Natural and artificial sources and their implications. *Environmental Engineering and Management Journal*, *9*, 881-888.

Sandu, I., Chirazi, M., Canache, M., Sandu, G.I., Alexeianu, M.T., Sandu, V.A., & Vasilache, V. (2010c). Research on NaCl saline aerosols II. New artificial halochamber characteristics. *Environmental Engineering and Management Journal*, *9*, 1105-1113.

Sandu, I., Canache, M., Lupascu, T., Chirazi, M., Sandu, I.G., & Pascu, C. (2013). The influence of physically doping NaCl with other salts on aerosol and solion generation, *Aerosol and Air Quality Research*, *10*, 1731-1740.

Smaldone, G.C., Walser, L., Perry, R.J., Ilowite, J.S., Bennett, W.D., & Greco, M. (1989). Generation and administration of aerosols for medical and physiological research studies. *Journal of Aerosol Medicine*, *2*, 81-87.

Sullivan, R.C., Moore, M.J.K., Petters, M.D., Kreidenweis, S.M., Roberts, S.M., & Prather, K.A. (2009). Effect of chemical mixing state on the hygroscopicity and cloud nucleation properties of calcium mineral dust particles. *Atmospheric Chemistry and Physics*, *9*, 3303-3316.

Stanier, C.O., Khlystov, A.Y., & Pandis, S.N. (2004). Ambient aerosol size distributions and number concentrations measured during the Pittsburgh Air Quality Study (PAQS). *Atmospheric Environment*, *38*, 3275-3284.

Tang, I.N. (1996). Chemical and size effects of hygroscopic aerosols on light scattering coefficients. *Journal of Geophysical Research*, *101*, 19245-19250.

Tang, P., Chan, H.K., Tam, E., de Gruyter, N., & Chan, J. (2006). Preparation of NaCl powder suitable for inhalation. *Industrial and Engineering Chemistry Research*, *45*, 4188–4192.

Wang, Z., King, S.M., Freney, E., Rosenoern, T., Smith, M.L., Chen, Q., Kuwata, M., Lewis, E.R., Poschl, U., Wang, W., Buseck, P.R., & Martin, S.T. (2010). The dynamic shape factor of sodium chloride nanoparticles as regulated by drying rate. *Aerosol Science and Technology*, *44*, 939-953.

Whitby, K.T. (1978). The physical characteristics of sulphur aerosols. *Atmospheric Environment*, *12*, 135-159.

Wise, M.E., Semeniuk, T.A., Bruintjes, R., Martin, S.T., Russel, L.M., & Buseck, P.R. (2007). Hygroscopic behaviour of NaCl-bearing natural aerosol particles using environmental transmission electron microscopy. *Journal of Geophysical Research*, *112*, D10224, doi: 10.1029/2006JD007678.

Xu, G.B., & You, C.P. (1985). Theoretical lung deposition of hygroscopic NaCl aerosols, *Aerosol Science and Technology*, *4*, 455-461.

Zangmeister, C.D., Turner, J.A., & Pemberton, J.E. (2001). Segregation of NaBr in NaBr/NaCl crystals grown from aqueous solutions: Implications for sea salt surface chemistry (Paper 2000GL012539). *Geophysical Research Letters*, *28*, 995-998.

Zelenov, V.V., Aparina, E.V., Ivashin, S.V., & Gershenson, Y.M. (2008). Steady-state uptake of NO_3 on NaBr/NaCl, NaI/NaCl, $MgCl_2 \times 6H_2O$/NaCl, $MgBr_2 \times 6H_2O$/NaCl binary salt coatings. *Russian Journal of Physical Chemistry B*, *2*, 408-417.

Tabel 1: Details related to the regression line characteristics, correlation coefficient and emission/erosion rate (min^{-1}) corresponding to the first stage in the aerosol generation mechanism, as identified from Fig. 3.

Sample Code	Pure or doped NaCl salts	Param.	1st stage	k_e (min^{-1})	2nd stage	3rd stage
P_0	NaCl (100%)	RF	y = 8.38E-08x	8.38E-08	y = 3.15E-09x+2.82E-05	-
		r^2	0.99		0.94	
P_1	NaCl (95%)	RF	y = 1.94E-08x	1.94E-08	y = 2.30E-09x+1.40E-06	y = 5.16E-10x+2.54E-06
		r^2	0.98		0.99	0.99
	KCl (5%)	RF	y = 2.24E-08x	2.24E-08	y = 2.60E-09x+1.84E-06	y = 7.73E-10x+2.99E-06
		r^2	0.99		0.97	0.99
P_2	NaCl (95%)	RF	y = 1.59E-08x	1.59E-08	y = 9.51E-10x+1.19E-06	y = 1.61E-10x+1.73E-06
		r^2	0.98		0.99	0.99
	KI (5%)	RF	y = 6.15E-09x	6.15E-09	y = 6.18E-10x+4.93E-07	y = 3.29E-10x+6.65E-07
		r^2	0.98		0.99	0.99
P_3	NaCl (95%)	RF	y = 1.57E-08x	1.57E-08	y = 7.34E-10x+1.59E-06	y = 3.31E-09x-3.82E-07
		r^2	0.85		0.99	0.99
	KBr (5%)	RF	y = 9.89E-09x	9.89E-09	y = 6.25E-10x+1.03E-06	y = 1.14E-09x+2.58E-07
		r^2	0.85		0.99	0.98
P_4	NaCl (90%)	RF	y = 4.68E-09x	4.68E-09	y = 4.36E-10x+4.07E-07	y = 3.08E-10x+4.52E-07
		r^2	0.99		0.97	0.97
	KI (5%) KCl (5%)	RF	y = 1.06E-08x	*9.59E-09**	y = 1.25E-09x+9.94E-07	y = 1.20E-09x+5.13E-07
		r^2	0.99		0.98	0.99
P_5	NaCl (95%)	RF	y = 1.63E-08x	1.63E-08	y = 1.11E-09x+1.21E-06	y = 3.10E-10x+1.81E-06
		r^2	0.97		0.97	0.99
	$CaCl_2$ (5%)	RF	y = 7.29E-08x	7.29E-08	y = 7.47E-09x+5.92E-06	y = 2.31E-09x+1.00E-05
		r^2	0.99		0.96	0.98

Note: * - the value is derived for the sum of KI and KCl since in the ion chromatographic analysis K^+ ion was quantified.

Fig. 1

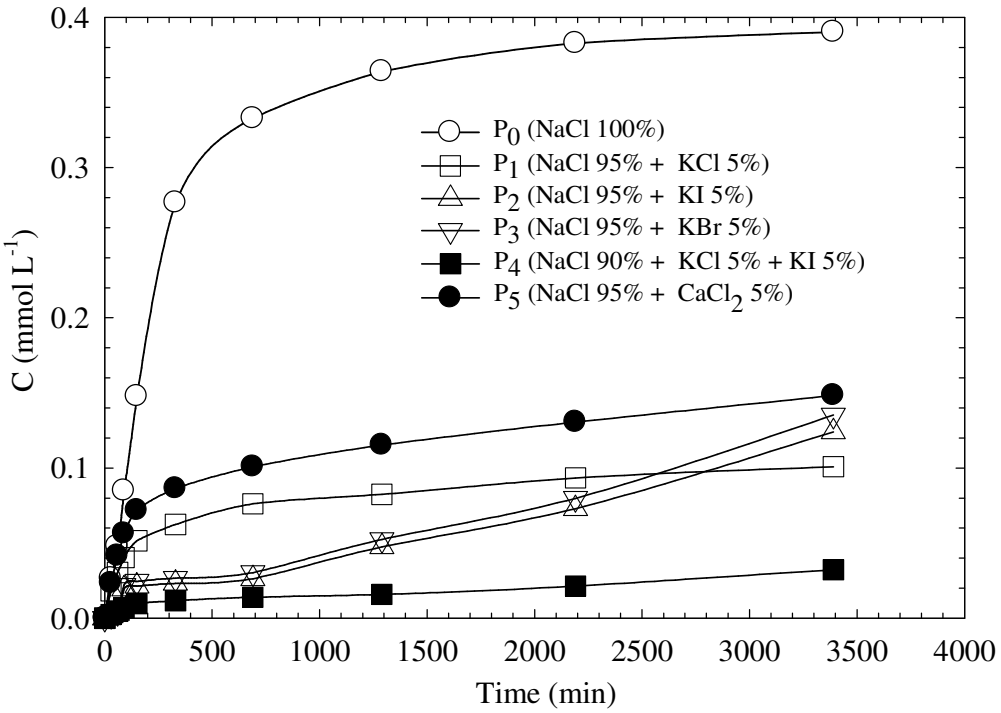

Fig. 1. Doping influence on saline aerosol generation from various active efflorescent salt mixtures: time trend of the aerosol concentration C (sum of the concentrations from the relevant cationic species in the solutions derived from the impinger).

Fig. 2

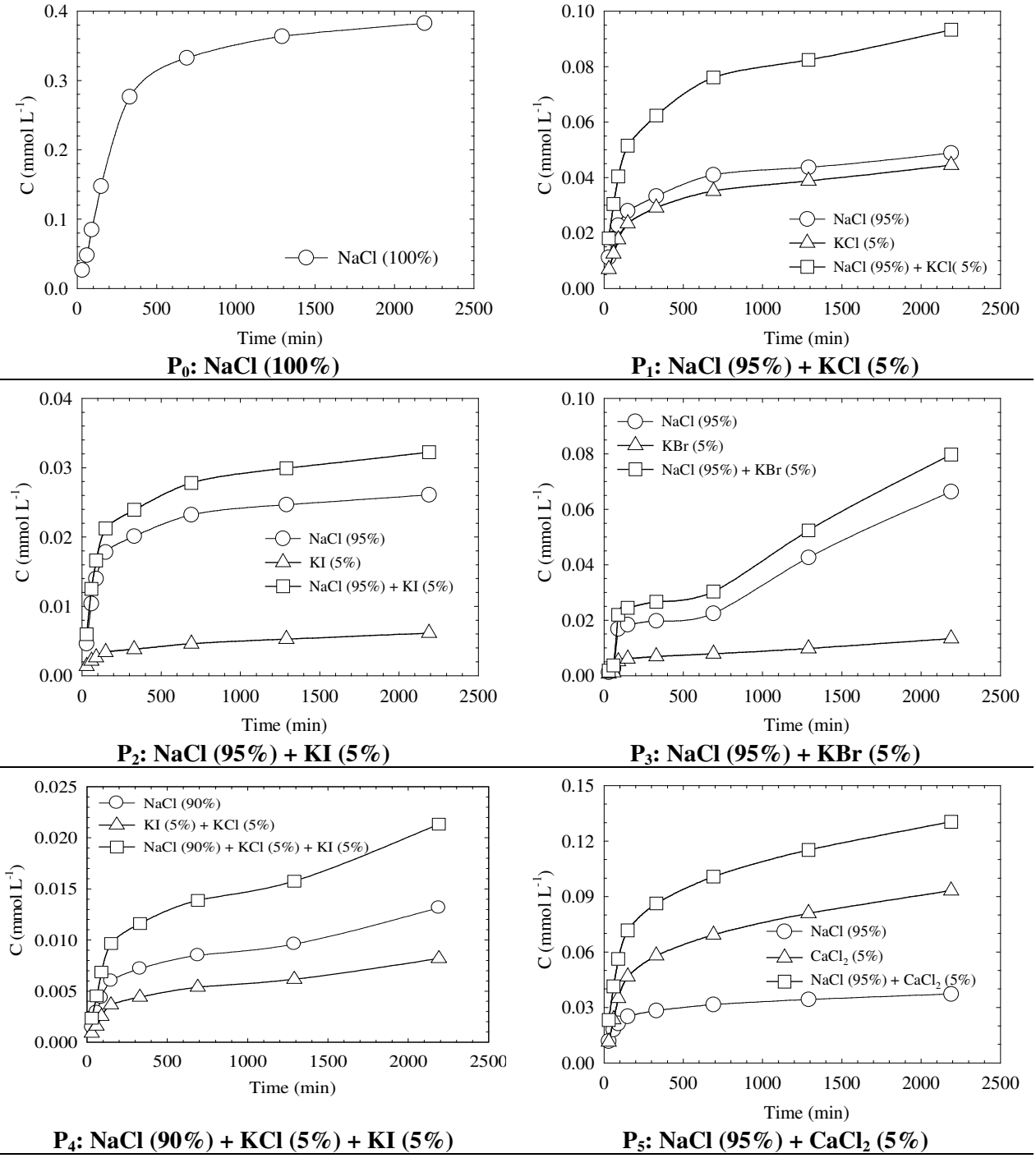

P_0: NaCl (100%) | **P_1: NaCl (95%) + KCl (5%)**

P_2: NaCl (95%) + KI (5%) | **P_3: NaCl (95%) + KBr (5%)**

P_4: NaCl (90%) + KCl (5%) + KI (5%) | **P_5: NaCl (95%) + $CaCl_2$ (5%)**

Fig. 2. Time evolution of the emission capacity both of each salt and their mixtures from various active efflorescent salt mixtures.

Fig. 3

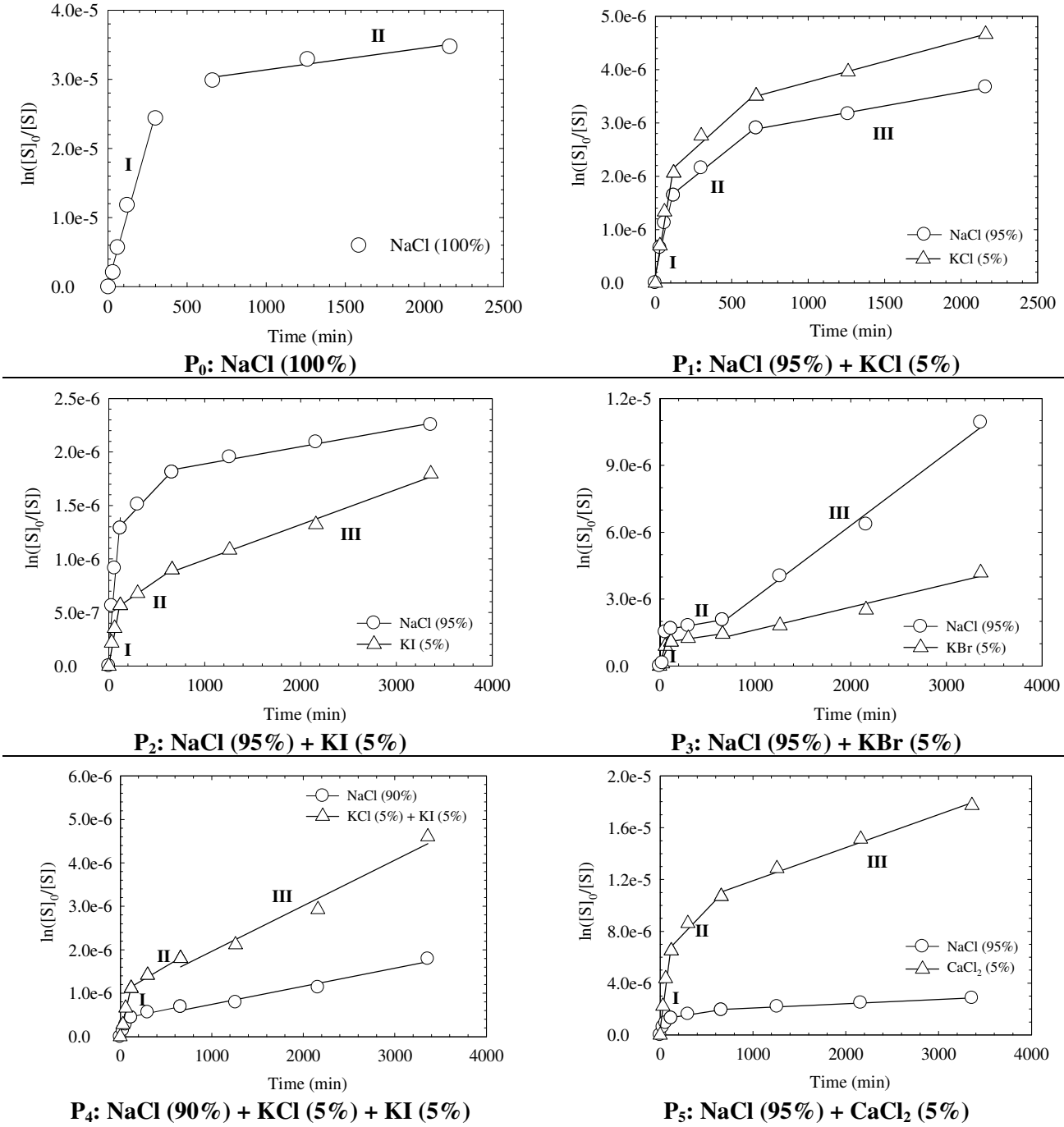

P_0: NaCl (100%) **P_1: NaCl (95%) + KCl (5%)**

P_2: NaCl (95%) + KI (5%) **P_3: NaCl (95%) + KBr (5%)**

P_4: NaCl (90%) + KCl (5%) + KI (5%) **P_5: NaCl (95%) + $CaCl_2$ (5%)**

Fig. 3. Profiles of the $\ln([S]_0/[S])$ vs. time curves specific for the investigated samples.